Talanta 127 (2014) 262–268

Contents lists available at ScienceDirect

Talanta

journal homepage: www.elsevier.com/locate/talanta

# An electrochemical sensor based on polyaniline for monitoring hydroquinone and its damage on DNA

Wenwei Tang [a,*], Min Zhang [b], Weihao Li [c], Xinping Zeng [b,*]

[a] Department of Chemistry, Tongji University, Shanghai 200092, China
[b] School of Life Science and Technology, Tongji University, Shanghai 200092, China
[c] Handan municipal centre for disease control and prevention, Handan, 056000, China

ARTICLE INFO

*Article history:*
Received 12 November 2013
Received in revised form
27 March 2014
Accepted 29 March 2014
Available online 5 April 2014

*Keywords:*
Biosensor
Polyaniline
Hydroquinone
Insert interaction
DNA damage

ABSTRACT

A dsDNA/PANI/CTS/GCE biosensor was constructed by using the biocompatible chitosan (CTS) and the polyaniline (PANI) with excellent electric catalytic properties and large specific surface areas. The electrochemical behavior of hydroquinone on biosensor and its DNA-damaging mechanisms were investigated. Results showed that the redox peak current was remarkably increased after glassy carbon electrode (GCE) was modified by PANI/CTS. The dsDNA damage by hydroquinone was concentration dependent, and increased along with the increase of hydroquinone oxidation peak current and the reduction of dsDNA guanine oxidation peak current. The linear detection range of hydroquinone with dsDNA/PANI/CTS/GCE was $1.25\times10^{-6}$–$3.2\times10^{-4}$ M, and the detection limit was $9.65\times10^{-7}$ M. It was confirmed by the UV method that applying dsDNA/PANI/CTS/GCE to monitor hydroquinone was accurate and reliable. In addition, it could be deduced that the mode of interaction between the hydroquinone and dsDNA was intercalation. The electrochemical oxidation of hydroquinone on the dsDNA/PANI/CTS/GCE electrode was an adsorption-controlled irreversible and a two-electron two-proton transfer process.


## 1. Introduction

Hydroquinone is a widely used chemical contained in cosmetics, medicines, environment, and human diet [1] and can be metabolized to benzoquinones which are potentially haematotoxic, genotoxic and carcinogenic compounds. It is a highly reactive molecule and can produce reactive oxygen species through redox cycle [2], resulting in DNA damage, mutation in cellular transformation and vivo tumourigenesis [3–5].

DNA stores genetic information for organism survival and reproduction, so it is crucial to maintain the integrity of DNA of the cell [6,7]. Some internal factors as well as external environment could cause damage to the DNA [8–11]. If the damaged DNA cannot be repaired in time, the induced gene mutation could result in a cancer or tumor [12,13]. Therefore, it is necessary to establish a sensitive, rapid, and inexpensive method to detect DNA damages.

For detecting the DNA damage, many analytical methods have been developed, including mass spectrometry [14], fluorescence [15], chromatography [16] and capillary electrophoresis [17]. However, these methods are either laborious or time consuming, involving complicated pretreatment, expensive instruments and long analysis time. Recently, electrochemical sensors or DNA biosensors, which are constructed based on electroactive polymers and nanophase materials, overcome these limitations and can provide a sensitive, direct, simple, and the rapid method to detect DNA damage. They could reflect the DNA damage by monitoring the changes of voltage (current) through the electrode surface [18–21] or by DNA dosimetric evaluation [22]. Nanomaterials such as carbon nanotubes (CNTs) [23] and nanostructured fiber arrays [24] have been found to promote the direct electrochemical response of DNA. CNTs-based DNA sensor could provide a sensitive voltammetric response for monitoring phenol pollutants [25].

Polyaniline (PANI), when used as a typical conducting polymer to establish biosensors, has been a research hotspot over the past few years [26] because of its structural diversification, unique doping mechanism, good environmental stability and simple synthesis [27–29]. The conjugated structure exists in the PANI molecule, so the electron has a high degree of transferability. Lee et al. [30] modified the GOx with functionalised PANI and a multiwalled carbon nanotube and accomplished the direct electrochemistry of an enzyme sensor. Dhand et al. [31] found that the GOx showed a good electrochemical activity after being wrapped by nanoscale electro-deposition PANI, which indicated that the PANI has a good biocompatibility.

* Corresponding authors.
*E-mail addresses:* tangww@tongji.edu.cn (W. Tang), zengxp@tongji.edu.cn (X. Zeng).

http://dx.doi.org/10.1016/j.talanta.2014.03.069
0039-9140/

Chitosan (CTS) is a kind of natural high-polymer material with great physicochemical and film-forming properties. It has chelation and adsorption abilities to many ions, organics and biomolecules, and has been used to prepare composite materials by the electrostatic self-assembly method [32].

Small molecules interact with DNA mainly by non-covalent interactions including electrostatic binding, groove binding and intercalation combination. Wang et al. [33] discovered that nicotine combined with DNA by electrostatic interaction and displayed an irreversible behavior on DNA/GCE electrodes. Shen et al. [34] found that DNA caused the reduction peak current of melamine to decrease and the peak potential to shift negatively. It was speculated that melamine combined with DNA by groove binding. Li et al. [35] reported that DNA resulted in a decrease of the mitoxantrone peak current, red shift and hypochromic effect, which indicated that intercalation was occurred between mitoxantrone and DNA.

In the present paper, the dsDNA/PANI/CTS/GCE biosensor was constructed, using PANI and CTS as modification materials of glassy carbon electrode (GCE). Cyclic voltammetry (CV), electrochemical impedance spectroscopy (EIS) and differential pulse voltammetry (DPV) were used to investigate the electrochemical behaviors of hydroquinone on the biosensor, as well as its damage mechanisms on dsDNA. Meanwhile, the linear range and detection limit of the biosensor for hydroquinone were investigated. This study provided a valuable method to construct biosensors for monitoring hydroquinone and its damage on DNA, which would have widely applications in the fields of environment and life sciences.

## 2. Experimental

### 2.1. Chemicals and materials

Working electrode was GCE (GC130, $\Phi$ 3 mm) developed by Tianjin Aida HengSheng technology development Co., Ltd. (Tianjin, China). Aniline, CTS, potassium ferricyanide, hydroquinone, sodium acetate were all of analytical grade and purchased from Sinopharm Chemical Reagent Co., Ltd. (Shanghai, China). Herring sperm double-stranded DNA was of biochemical level and purchased from Sigma Co. (St. Louis, MO, US).

### 2.2. Preparation of PANI modified materials

0.9 mL of aniline (ANI) monomer and 0.84 g of activated carbon powder were dispersed in 30 mL of 1 M hydrochloric acid solution. Nitrogen gas was inlet to remove oxygen for 30 min. The solution was stirred at a constant speed for 1 h to make the aniline monomer uniformly adsorbed on the surface of the activated carbon. A certain amount of ammonium persulfate (APS) was dissolved in 20 mL of hydrochloric acid solution (1 M) under the nitrogen gas flow. The prepared APS hydrochloric acid solution was added dropwise to the above aniline hydrochloric acid solution within 1 h under the reaction temperature of 0 °C, and the reaction was maintained uniformly stirring for 5 h. After the reaction, the sample was repeatedly washed and filtered with 1 M hydrochloric acid, ethanol and distilled water to remove the unreacted and incompletely reacted oligomers. Finally, the sample was dried in vacuum oven for 24 h at 60 °C, and a deep green PANI-modified material was obtained.

### 2.3. Pretreatment of GCE

Electrodes were polished on the alumina powders with particle diameters of 0.3, 0.1, 0.05 μm in 8 font grinding way. The polished electrode was placed in the nitric acid solution with a volume ratio of 1:1 for 20 min, and then ultrasonically washed with distilled water, ethanol and distilled water successively. The treated electrode was put into 80 ml of 0.2 M KCl and 5 mM $K_3[Fe(CN)_6]$ solution to scan the CV. If the results met the standard ($\Delta E_p < 80$ mV), the electrode was washed with bidistilled water for future use.

### 2.4. Preparation of modified electrodes

CTS/GCE electrode: 1% (w/w) acetic acid (HAc) solution was prepared, and a certain amount of CTS was dissolved to obtain 0.7% (w/v) CTS-HAc solution, ultrasonically treating until it became uniform and transparent. The GCE was evenly coated with 10 μL of the CTS-HAc solution and dried at room temperature.

PANI/CTS/GCE electrode: A certain amount of PANI was added into the above prepared CTS-HAc solution and treated with ultrasound for 3 min to mix them evenly, obtaining a 1 mg/mL of PANI/CTS dispersion. The GCE was evenly coated with 10 μL of the dispersion and dried at room temperature.

DsDNA/PANI/CTS/GCE electrode: a certain amount of herring sperm double-stranded DNA was dissolved in Tris–HCl solution to obtain a 9 mg/mL DNA solution. The surface of PANI/CTS/GCE was evenly coated with DNA and stored in the refrigerator at 4 °C overnight for drying and future use.

### 2.5. SEM analysis

A S-4800 field emission scanning electron microscope (SEM) from Hitachi Ltd. (Toyoko, Japan) with cold filed electron emission source, 0.5–30 kV accelerating voltage and 5–80 k magnification was used in the experiments.

### 2.6. Electrochemical tests

Autolab model PGSTAT30 electrochemistry workstation was used to test electrochemical properties of the electrode. The prepared electrode was used as working electrode, a platinum electrode was as the counter electrode, and a silver silver–chloride electrode was used as the reference electrode.

For the cyclic voltammetry (CV) test, the sweep speed was set as 50 mV $s^{-1}$ and the scanning range was −0.1 to 0.6 V. For the EIS test, the frequency range was 10000–0.1 Hz and the electric potential of the amplitude was 50 mV. The modulation amplitude for DPV test was 0.05 V, the waiting potential was 0 V, the time interval was 0.2 s, $d$ the pulse time was 0.05 s and the scan rate was 25.5 mV $s^{-1}$.

### 2.7. Monitoring hydroquinone degraded by $H_2O_2$ and UV

Hydroquinone was degraded by combination of $H_2O_2$ and UV in a quartz tube. The UV lamp power was 15 W, and the maximum emission wavelength was 253.7 nm. The initial concentrations of hydroquinone and $H_2O_2$ were $5.00 \times 10^{-5}$ M and 0.10 M, respectively. After 30 min degradation, hydroquinone was measured by both electrochemical method and UV–visible spectrophotometry, and the degradation rate was calculated.

## 3. Results and discussion

### 3.1. SEM of PANI composite

The aggregation morphology of PANI particles attached to the activated carbon was shown in Fig. 1(a). The activated carbon particles were packed tightly and thus increased the loads of PANI.

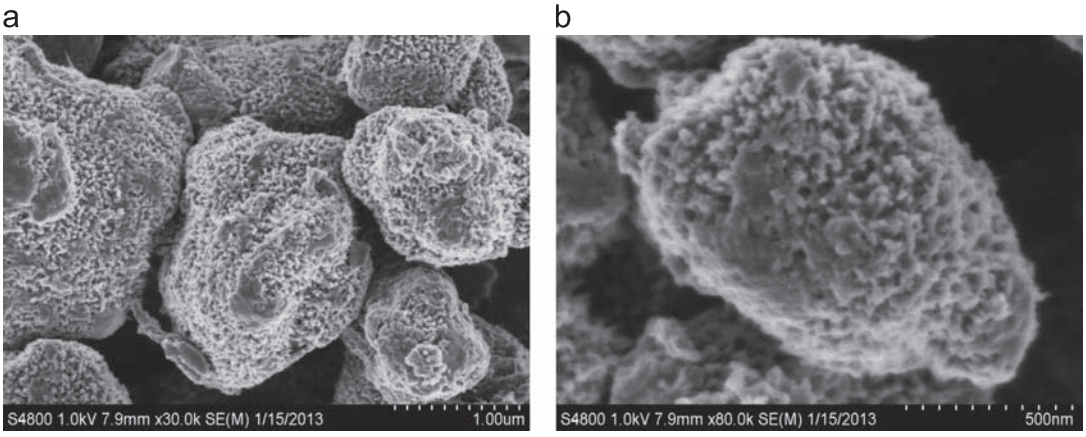


**Fig. 1.** SEM of PANI composite materials. (a) ×30 k and (b) ×80 k.

The PANI had porous structure and dispersed on the surface of the activated carbon particles as tiny particles (Fig. 1(b)). A mesh structure was formed by mutual particles bridging. The smaller the PANI particles, the larger the surface areas, and the greater the contact areas between polymers and ions in the medium, which was favored for charge transfer.

### 3.2. Construction of dsDNA/PANI/CTS/GCE

#### 3.2.1. CV of the dsDNA/PANI/CTS/GCE electrode

Both non-modified and modified electrodes exhibited reversible redox peaks (Fig. 2). The redox peak potentials of GCE were 0.213 V and 0.285 V, and $\Delta E_p$ was 72 mV, smaller than 80 mV. This indicated that the negative impediment of GCE to electron transportation or electrode reaction was relatively small.

Comparing curve (a and b), the redox current of $K_3[Fe(CN)_6]$ on electrode (b) was slightly enlarged after CTS modification. This was probably because that $[Fe(CN)_6]^{3-}$ was attracted by the positively charged amino groups on CTS via electrostatic interaction. The accumulated $[Fe(CN)_6]^{3-}$ on the surface of electrode and (b) resulted a larger redox current.

The redox current on electrode (c) was remarkably enhanced in comparison with electrode (a and b). On one side, PANI composite was highly conductive materials, which could enhance the electric signal of the electrode, and the electrode sensitivity. On the other side, the larger specific area of PANI increased the attachment of $K_3[Fe(CN)_6]$ on the electrode.

Comparing curve (d) and (c), the redox peak current of dsDNA/PANI/CTS/GCE was slightly dropped which was primarily because of the poor electron transfer capability of dsDNA. As the dsDNA contained negatively-charged DNA phosphate backbone, which excluded the negatively-charged $[Fe(CN)_6]^{3-}$ from the electrode surface, the electron transfer on the surface of the electrode was hindered, so the redox peak current of electrode (d) dropped.

#### 3.2.2. Impedance of the dsDNA/PANI/CTS/GCE electrode

As shown in Fig. 3, the impedance values of electrode (a–c) were decremented in the high frequency region. After the modification of CTS and PANI–CTS, the CTS electrostatic adsorption and the strong PANI conductive ability increased the redox currents of the modified electrodes, while reducing the surface resistance of the GCE. Comparing curve (d and c), the DNA-modified electrode displayed a significantly increased curvature of the semi-curve in the high frequency region.

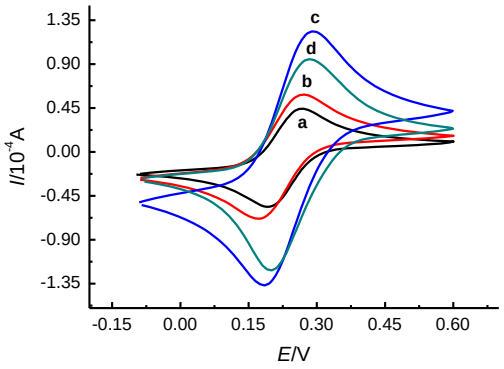


**Fig. 2.** The CV of different modified electrodes in the 0.2 M KCl solution containing $5 \times 10^{-3}$ M $K_3$ [Fe (CN)$_6$]. (a) GCE, (b) CTS/GCE, (c) PANI/CTS/GCE and (d) DNA/PANI/CTS/GCE.

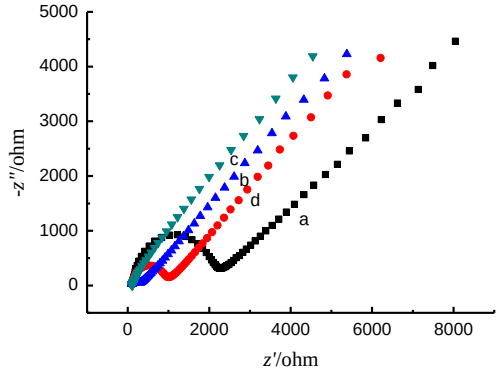


**Fig. 3.** The EIS of different modified electrodes in the 0.1 M KCl solution containing $5 \times 10^{-3}$ M $K_3$ [Fe(CN)$_6$]/$K_4$[Fe(CN)$_6$] (1:1). (a) GCE, (b) CTS/GCE, (c) PANI/CTS/GCE and (d) DNA/PANI/CTS/GCE.

The drop of the redox peak current and increase of the surface resistance of DNA/PANI/CTS/GCE indicated effective modification of the PANI/CTS/GCE electrode by dsDNA.

### 3.3. Elecchemial behaviors of dsDNA on different modified electrodes

The oxidation peak potential of dsDNA was about 0.9 V which represented the oxidation peak of guanine in the dsDNA (Fig. 4).

The oxidation peak of the dsDNA/GCE at 0.9 V was not obvious because the dsDNA was directly modified on the surface of GCE, which had low adhesion ability, and caused difficulties in the

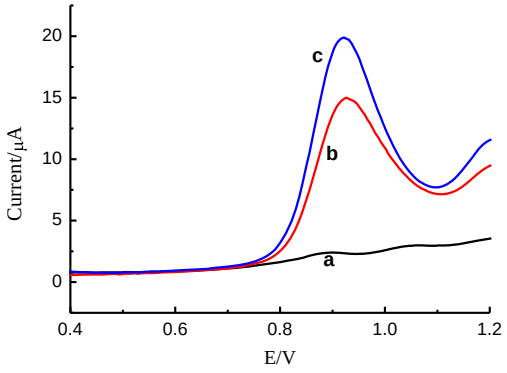


**Fig. 4.** Electrochemical behaviors of dsDNA on different modified electrodes in 0.2 M HAc buffer (pH=4.4). (a) dsDNA/GCE, (b) dsDNA/CTS/GCE and (c) dsDNA/PANI/CTS/GCE.

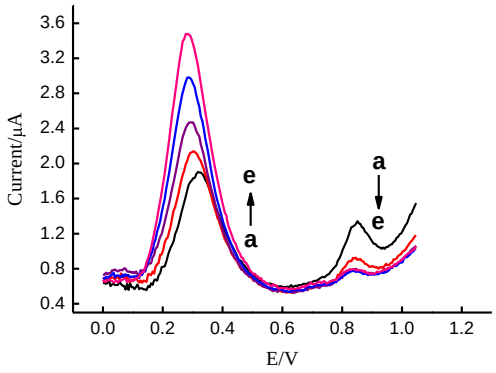


**Fig. 5.** DsDNA/PANI/CTS/GCE interaction with different concentrations of hydroquinone for 6 min in HAc buffer. (a) $2.5\times10^{-5}$ M, (b) $5.0\times10^{-5}$ M, (c) $7.5\times10^{-5}$ M, (d) $10.0\times10^{-5}$ M and (e) $12.5\times10^{-5}$ M.

electron transfer between the internal guanine of the dsDNA double helix and the GCE.

The peak current of the dsDNA/CTS/GCE electrode was greater than that of the dsDNA/GCE electrode. Because CTS had good biocompatibility with the biological macromolecules dsDNA, they had good complementary connection, which increased the fixed amount of dsDNA on the CTS/GCE. Moreover, CTS contained a large amount of amino groups, which increased the charge transfer capability of the dsDNA/CTS/GCE electrode.

The oxidation peak current of the dsDNA/PANI/CTS/GCE electrode was the largest, indicating that the GCE modified by both CTS and PANI composite showed better electrochemical response. On one hand, PANI had excellent electro-catalysis performance, which could serve as a powerful amplifier to enhance the dsDNA response signal. On the other hand, the PANI modification increased the surface area of the electrode, and thus increased the adsorption of dsDNA, further enhancing the dsDNA response signal.

### 3.4. Damage on dsDNA by hydroquinone

As shown in Fig. 5, each curve contained two oxidation peaks at about 0.3 V and 0.85 V, which represented the oxidation of hydroquinone and guanine in the dsDNA, respectively. The oxidation peak current of hydroquinone showed an increasing trend along with the gradually increased concentrations ($a\rightarrow e$), while that of the guanine in the dsDNA reduced continuously. With the increase of hydroquinone, the amount of embedded hydroquinone in the double helix of dsDNA was gradually increased, causing more serious damage to the dsDNA. As a result, the redox reactions of bases

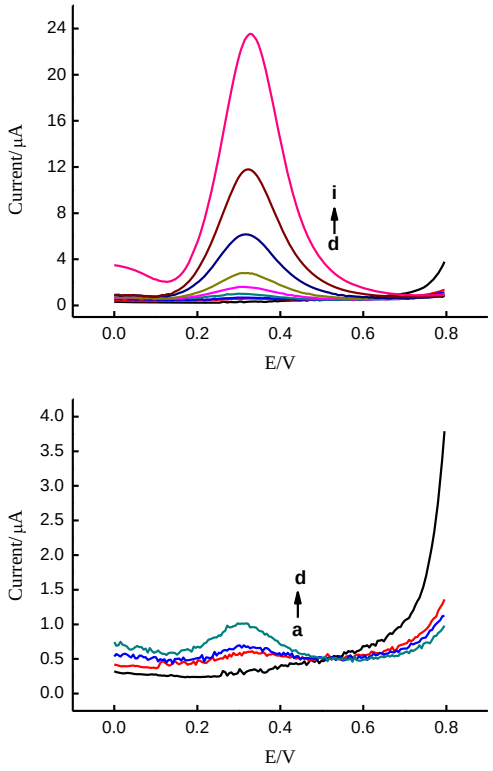


**Fig. 6.** The responses of the dsDNA/PANI/CTS/GCE electrode in 0.2 M HAc buffer (pH=4.4) with different concentrations of hydroquinone. (a) $1.25\times10^{-6}$ M, (b) $2.5\times10^{-6}$ M, (c) $5.0\times10^{-6}$ M, (d) $1.0\times10^{-5}$ M, (e) $2.0\times10^{-5}$ M, (f) $4.0\times10^{-5}$ M, (g) $8.0\times10^{-5}$ M, (h) $1.6\times10^{-4}$ M and (i) $3.2\times10^{-4}$M.

were hindered and the oxidized guanine reduced, thus, the oxidation peak current became lower.

### 3.5. Detection limit of dsDNA/PANI/CTS/GCE on hydroquinone

To calculate the detection limit, the following formula was used:

$$DL=\frac{3.3\ s}{k} \quad (1)$$

where $DL$ was the detection limit, $s$ was the sample standard deviation, and $k$ stranded for the slope of the linear fitting curve of the hydroquinone electrochemical oxidation current and concentration.

The responses of different concentrations of hydroquinone in HAc buffer on the dsDNA/PANI/CTS/GCE electrode were shown in Fig. 6.

The oxidation peaks of hydroquinone were observed at around 0.3 V. With the increase of hydroquinone concentration, the oxidation peak current showed a continuously increasing trend. The concentration of hydroquinone was set as the $x$ coordinate and the oxidation peak current of hydroquinone was set as the $y$ coordinate. The result showed that when the concentration of hydroquinone was in the range of $1.25\times10^{-6}$–$3.2\times10^{-4}$ M, the oxidation current of hydroquinone had a linear relationship with its concentration. The fitting equation of the oxidation current and concentration was

$$y=0.00853x+1.11766\times10^{-6},\quad (R^2=0.99804) \quad (2)$$

The dsDNA/PANI/CTS/GCE electrode was repeatedly tested for eight times in HAc buffer containing hydroquinone. The calculated standard deviation was $2.49043\times10^{-9}$. Put the standard deviation and the working slope into Eq. (1), the linear range of the dsDNA/PANI/CTS/GCE electrode to hydroquinone was obtained as $1.25\times10^{-6}$–$3.2\times10^{-4}$ M. The detection limit was $9.65\times10^{-7}$ M.

Based on the experimental evidence, we can conclude that dsDNA/PANI/CTS/GCE electrode exhibited superior sensing ability and current sensitivity. The result is comparable with other's work [36–40] as illustrated in Table 1.

### 3.6. Monitoring hydroquinone after degradation

The interactions of the dsDNA with the non-degraded and degraded hydroquinone were shown in Fig. 7. After degradation for 30 min, the oxidation peak current of hydroquinone at about 0.3 V decreased obviously, while the oxidation peak current of guanine at around 0.85 V was significantly increased. This was because the previous interacted dsDNA was released as the degradation of hydroquinone, thereby caused the oxidation peak current of dsDNA increase.

According to the reduction of the hydroquinone oxidation peak current, the hydroquinone degradation rate could be obtained as 34.7%.

To evaluate the reliability of the method, the absorbance of hydroquinone at the maximum absorption wavelength before and after degradation was measured by UV–vis spectrophotometer (Table 2).

According to the absorbance, the hydroquinone degradation rate was 33.3%. The degradation rates based on the above two testing methods were almost the same, and the relative error was 4.0%. Therefore, the method using the dsDNA/PANI/CTS/GCE to detect the hydroquinone degradation was reliable.

### 3.7. Test of simulated water samples

Fetching tap water, treated with 0.45 μm membrane filter for the elimination of $Cu^{2+}$, $Mg^{2+}$, $A1^{3+}$, $Fe^{3+}$ interference, adding an appropriate amount of EDTA before the test. No hydroquinone was detected by dsDNA/PANI/CTS/GCE. Afterwards, add a certain amount of hydroquinone for simulated water samples, and using the recovery of standard addition method to test the hydroquinone concentration in simulated wastewater and doing three parallel samples. The experimental results are shown in Table 3. Using dsDNA/PANI/CTS/GCE to detect hydroquinone concentration in samples, the recovery rate was between 96% and 102.3%, and the relative standard deviation ranged in 0.9–3.3%, therefore the method can be used for the determination of practical samples.

**Table 1**
Comparison of the responses of some hydroquinone sensors constructed based on different modified electrode materials

| Electrode materials | Technique | Detection limit (μmol $L^{-1}$) | Linear range (μmol $L^{-1}$) | Ref. |
|---|---|---|---|---|
| Penicillamine | DPV | 1 | 15–115 | [36] |
| CNx | LSV | 1.2 | 10–1000 | [37] |
| Graphene | DPV | 0.8 | 1–10 and 10–80 | [38] |
| MWNTs | LSV | 0.6 | 2–100 | [39] |
| LDHf | DPV | 9 | 12–800 | [40] |
| Polyaniline | DPV | 0.96 | 1.25–320 | This work |

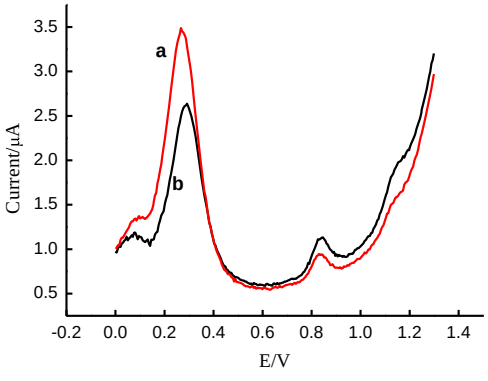


**Fig. 7.** Monitoring hydroquinone treated by $H_2O_2$ and UV in 0.2 M HAc buffer (pH=4.4). (a) Control sample and (b) treated for 30 min.

**Table 2**
The UV absorbance of hydroquinone

| No. | Sample | Absorbance |
|---|---|---|
| 1 | Before degradation | 0.63 |
| 2 | After degradation | 0.42 |

**Table 3**
Recoveries of hydroquinone with different concentrations

| No. | Added content (μM) | Determined content (μM) | Recovery (%) | RSD (%) |
|---|---|---|---|---|
| 1 | 20 | 19.2 | 96.0 | 0.9 |
| 2 | 100 | 97.6 | 97.6 | 3.3 |
| 3 | 200 | 204.6 | 102.3 | 1.7 |

### 3.8. Interation pattern between dsDNA and hydroquinone

#### 3.8.1. DPV study on the interaction

As shown in Fig. 8, without specific materials in the HAc buffer solution, the DPV of the PANI/CTS/GCE was smooth.

The PANI/CTS/GCE was scanned in the hydroquinone buffer, and the oxidation peak showed up at 0.226 V. Comparing the curves of (a and b), as only hydroquinone was added in (b), it could be determined that the peak at 0.226 V was the oxidation peak of hydroquinone on the electrode.

Comparing the curves of (b and c), the oxidation peak potential of curve (c) appeared at 0.358 V, which was obviously moved to the right and the current peak value was decreased. The electrode (c) was modified with dsDNA on the basis of the electrode (b), so it indicated that when dsDNA was present, the oxidation peak potential of hydroquinone moved to the right and the oxidation peak value decreased.

According to the reference [41], when small molecules interacted with DNA, the oxidation peak potential moved to the right, it indicated the interaction mode between the substances and the DNA was intercalation. Therefore, the binding mode between dsDNA and hydroquinone was preliminarily determined as intercalation.

#### 3.8.2. Influence of the ionic strength on the interaction

According to the theory proposed by Erdem et al. [42], when small molecules were embedded into the dsDNA, they were less affected by the ionic strength due to the protective effect of skeleton and phosphate base pairs. However, when the small molecules interacted with the dsDNA through electrostatic interaction, because the cations could bind to the negatively charged phosphate backbone and competed with the small molecules, the electrochemical signal was changed correspondingly.

As shown in Fig. 9, the hydroquinone oxidation peak potential and the current at 0.4 V varied little, and the guanine oxidation peak at 0.85 V was not changed much, either. Therefore, it demonstrated that the interaction between dsDNA and hydroquinone was intercalation rather than the electrostatic interaction.

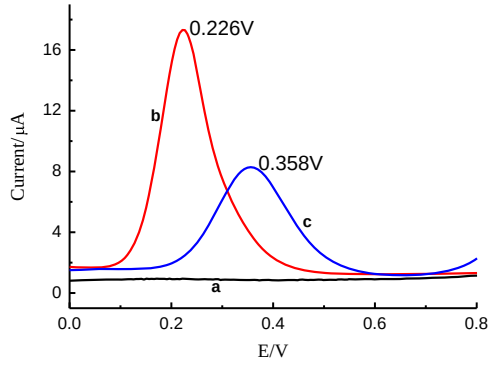


**Fig. 8.** The DPV of different modified electrodes in different solutions. (a) PANI/CTS/GCE in HAc buffer, (b) PANI/CTS/GCE in HAc buffer containing $1.3\times10^{-4}$ M hydroquinone and (c) dsDNA/PANI/CTS/GCE in HAc buffer containing $1.3\times10^{-4}$ M hydroquinone.

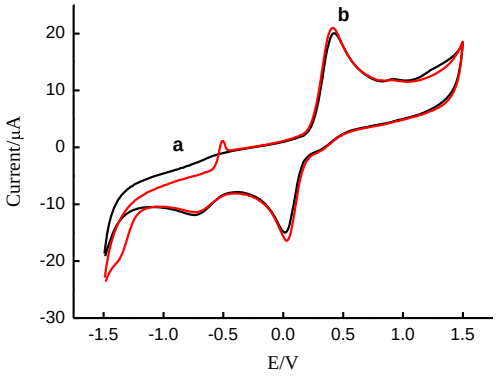


**Fig. 9.** The influence of $Na^+$ on CV of the dsDNA/PANI/CTS/GCE interact with $7.5\times10^{-4}$ M hydroquinone in HAc buffer. (a) without NaCl and (b) with 0.03 M NaCl.

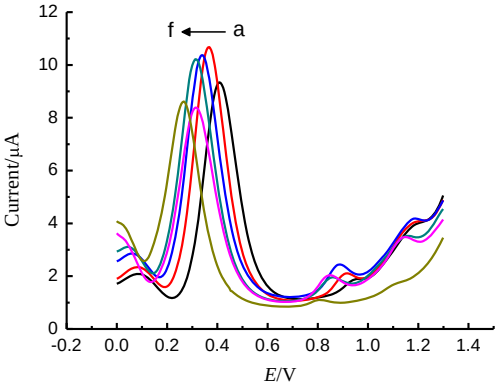


**Fig. 10.** DsDNA/PANI/CTS/GCE interact with hydroquinone ($7.5\times10^{-5}$ M) in acetic acid buffer with different pH. (a) 3.6, (b) 4.0, (c) 4.4, (d) 4.8, and (e) 5.2.

### 3.9. Mechanism study of hydroquinone and dsDNA interaction

#### 3.9.1. Impact of pH on the dsDNA–hydroquinone interaction

The values of the equilibrium potential implicate the redox activities of substances, which can be used to determine the possibility of electrochemical reaction. For the reactions involving protons and electrons, the electrode potential varies along with the changes of the solution pH value.

As shown in Fig. 10, when the solution pH increased from 3.6 to 5.2, the oxidation potential of hydroquinone moved towards the more negative direction.

Using the buffer solution pH as abscissa and the hydroquinone oxidation peak potential as ordinate, the curve was drawn, as well as the linear fit to the peak potential and pH value, the fitting equation was as follows:

$$E/V = 0.6286 - 0.064\ \text{pH}, \quad (R^2 = 0.9523) \tag{3}$$

The slope was determined as 64 mV $pH^{-1}$ by the linear equations, which was close to the ideal 59 mV $pH^{-1}$ (25 °C), suggesting that equal protons and electrons were involved in the interaction between hydroquinone and DNA in the electrochemical oxidation process on the dsDNA/PANI/CTS/GCE modified electrode. This result was similar to the previous work reported by Luckza [43].

#### 3.9.2. Impact of scan rate on the dsDNA–hydroquinone interaction

It is known that electroactive substances firstly reach the electrode surface through diffusion, and then adsorbed on the electrode surface to get involved in the reaction. The slower one of these two steps controls the reaction. If the peak current is linear to the scan rate, the electrochemical reaction is of adsorption control, and if the peak current is linear to the scan rate square, the reaction is of diffusion control [44].

The CV curves of hydroquinone on the dsDNA/PANI/CTS/GCE were shown in Fig. 11. As the scan rate increased gradually from 20 to 120 mV $s^{-1}$, the oxidation peak current increased. Using the scan rate as abscissa and the hydroquinone oxidation peak current as ordinate, the linear fitting equation of the hydroquin one electrochemical oxidation current and the scan rate was as follows:

$$i/(\mu A) = 0.1v/(\text{mV s}^{-1}) + 2.0, \quad (R^2 = 0.98) \tag{4}$$

According to the fitting results, there was a linear relationship between the oxidation peak current and the scan rate, indicating that the electrochemical oxidation of hydroquinone on the dsDNA/PANI/CTS/GCE electrode was controlled by the adsorption process. Moreover, there was a large shift of the redox peak potential along with the increase of scan rate, which suggested that the electrode reaction was an irreversible process. In summary, hydroquinone and DNA interaction was an adsorption-controlled irreversible process.

According to a report from Laviron [45], for a completely irreversible electrochemical oxidation process controlled by adsorption, the oxidation peak potential was defined by the following equation:

$$E_p = E^\circ + \left(\frac{RT}{\alpha nF}\right)\ln\left(\frac{RTk_s}{\alpha nF}\right) + \left(\frac{RT}{\alpha nF}\right)\ln v \tag{5}$$

where $E_p$ was for the oxidation peak potential of the substrate (V), $E^\circ$ was for the potential (V), $k_s$ was for the electrochemical rate

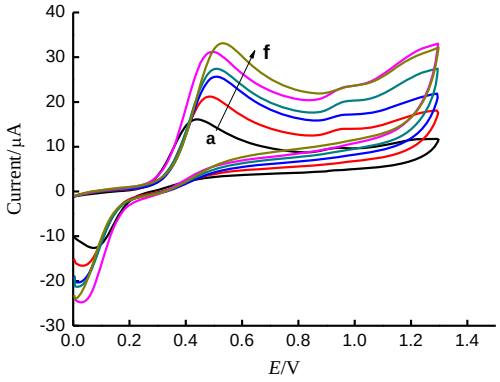


**Fig. 11.** The CV of dsDNA/PANI/CTS/GCE electrode in acetic acid buffer with $7.5\times10^{-5}$ M hydroquinone with different sweep speed. (a) 20 mV $s^{-1}$, (b) 40 mV $s^{-1}$, (c) 60 mV $s^{-1}$, (d) 80 mV $s^{-1}$, (e) 100 mV $s^{-1}$, and (f) 120 mV $s_{\circ}^{-1}$

constant, $\alpha$ was for the electron transfer coefficient of the electrode reaction, $n$ was for the electron transfer number of the oxidation reaction, and $\nu$ was for the scanning rate.

To calculate the number of electron transfer, it should fit the relationship between the ln $\nu$ and the potential.

Experimental results showed that the oxidation peak potentials of hydroquinone all displayed positive shift with increasing scan rate. There was also a linear relationship between the oxidation peak potential and ln$\nu$, of which the fitting equation was as follows:

$$E_p/\mathrm{V} = 0.0476 \ln \nu/(\mathrm{mV\ s^{-1}}) + 0.3032, \quad (R^2 = 0.97) \tag{6}$$

Based on the Eqs. (5) and (6), it could be determined that $\alpha n = 0.69$. For an irreversible electrochemical process, usually $0.3 < \alpha < 0.7$ [46], meanwhile, the structure of hydroquinone was symmetric, thus it could be obtained that $\alpha = 0.35$, $n = 2$.

Combining the relationship of pH and oxidation peak potential, it implied that the electrochemical oxidation of hydroquinone on dsDNA/PANI/CTS/GCE modified electrode was a two-electron two-proton transfer process.

## 4. Conclusions

The GCE was successfully modified by CTS, which has excellent biocompatibility, and PANI, which has excellent electro-catalysis performance and large surface areas. The redox peak currents of the modified electrode increased remarkably. With the gradual increase of hydroquinone concentration, its damage on the dsDNA was aggravated, the oxidation peak current of hydroquinone increased and the oxidation peak current of guanine decreased continuously. Using the dsDNA/PANI/CTS/GCE electrode to detect hydroquinone, the linear range was $1.25 \times 10^{-6}$–$3.2 \times 10^{-4}$ M and the detection limit was $9.65 \times 10^{-7}$ M. The interaction mode between dsDNA and hydroquinone was intercalation. The electrochemical oxidation of hydroquinone on the dsDNA/PANI/CTS/GCE electrode was an adsorption-controlled irreversible and a two-electron two-proton transfer process.

## Acknowledgments

This work was supported by the National Natural Science Foundation of China (No. 21277098), the Natural Science Foundation of Shanghai (No. 10ZR1432500), the Shanghai Municipal Commission of Economy and Informatization (No. 20122846).

## References

[1] D. Davidson, R. Courage, C. Rushton, L. Levy, Occup. Environ. Med. 58 (2001) 2–13.
[2] J. Bolton, M.A. Trush, T.M. Penning, G. Dryhurst, Chem. Res. Toxicol. 13 (2000) 135–160.
[3] L. Luo, L. Jiang, C. Geng, J. Cao, L. Zhong, Chem. Biol. Interact. 173 (2008) 1–8.
[4] D.J. Abernethy, E.V. Kleymenova, J. Rose, L. Recio, B. Faiola, Toxicol. Sci. 79 (2004) 82–89.
[5] K. Shosuke, H. Yusuke, M. Mariko, O. Shinji, Free Radic. Biol. Med. 32 (2002) 822–832.
[6] C. Céline, C. Marie, K. Marsolier, DNA Repair 8 (2009) 1101–1109.
[7] D. Ugo, Y. Jean, DNA Repair 6 (2007) 561–577.
[8] F. Gugliesi, M. Bawadekar, M. De Andrea, V. Dell'Oste, V. Caneparo, A. Tincani, M. Gariglio, S. Landolfo, Plos One 8 (2013) 1–11 (e63045).
[9] E.J. Petersen, B.C. Nelson, Anal. Bioanal. Chem. 398 (2010) 613–650.
[10] A. Ali, A. Maryam, R. Behzad, Sens. Actuators B: Chem. 177 (2013) 862–870.
[11] Y. Wang, H.Y. Xiong, X.H. Zhang, S.F. Wang, Sens. Actuators B Chem. 161 (2012) 274–278.
[12] Y. Liu, N. Hu, Biosens. Bioelectron. 25 (2009) 185–190.
[13] D.H. Zhang, Y. Cui, H.T. Shen, L.X. Xing, J.F. Cui, J. Wang, X.H. Zhang, Plos One 8 (2013) 1–11 (e65044).
[14] M. Tarum, B. Bajrami, J.F. Rusling, Anal. Chem. 78 (2006) 624–627.
[15] V. Viswesh, K. Gates, D. Sun, Chem. Res. Toxicol. 23 (2010) 99–107.
[16] A. Asan, I. Isildak, J. Chromatogr. A 988 (2003) 145–149.
[17] S. Dong, L. Chi, Z. Yang, P. He, Q. Wang, Y. Fang, J. Sep. Sci. 32 (2009) 3232–3238.
[18] A.A. Ensafi, B. Rezaei, M. Amini, E. Heydari-Bafrooei, Talanta 88 (2012) 244–251.
[19] T.L. Liao, Y.F. Wang, X.B. Zhou, Y. Zhang, X.H. Liu, J. Du, X.J. Li, X.Q. Lu, Colloids Surf. B 76 (2010) 334–339.
[20] M.Y. Wei, L.H. Guo, P. Famouri, Microchim. Acta 172 (2011) 247–260.
[21] M.F. Barroso, N. de-los-Santos-Álvarez, M.J. Lobo-Casta~nón, A.J. Miranda-Ordieres, C. Delerue-Matos, M.B.P.P. Oliveira, P. Tu~nón-Blanco, Biosens. Bioelectron. 26 (2011) 2396–2401.
[22] A.P. Schuch, J.C. Lago, T. Yagura, C.F.M. Menck, Plos One 7 (2012) 1–8 (e40344).
[23] G.A. Rivas, M.D. Rubianes, M.C. Rodriguez, N.F. Ferreyra, G.L. Luque, M. L. Pedano, S.A. Miscoria, C. Parrado, Talanta 74 (2007) 291–307.
[24] F. Deiss, N. Sojic, D.J. White, P.R. Stoddart, Anal. Bioanal. Chem. 396 (2010) 53–71.
[25] Y.Q. Zheng, C.Z. Yang, W.H. Pu, J.D. Zhang, Microchim. Acta 166 (2009) 21–26.
[26] A. Terbouche, C. Ait-Ramdane-Terbouche, Sens. Actuators B: Chem. 169 (2012) 297–304.
[27] K.P. Lee, S. Komathi, N.J. Nam, J. Microchem, A.I. Gopalan, Microchem. J. 95 (2010) 74–79.
[28] H. Bejbouji, L. Vignau, J.L. Miane, M.T. Dang, E.M. Qualim, M. Harmouchi, A. Mouhsen, Sol. Energy Mater. Sol. Cells 94 (2010) 176–181.
[29] C. Dhand, G. Sumana, M. Datta, Thin Solid Films 519 (2010) 1145–1150.
[30] K.P. Lee, S. Komathi, N.J. Nam, A.I. Gopalan, Microchem. J. 95 (2010) 74–79.
[31] C. Dhand, G. Sumana, M. Datta, B.D. Malhotra, Thin Solid Films 519 (2010) 1145–1150.
[32] R. Khan, A. Kaushik, P.R. Solanki, A.A. Ansari, M.K. Pandey, Anal. Chim. Acta 616 (2008) 207–213.
[33] L. Wang, H.Y. Xiong, X.H. Zhang, Electrochem. Commun. 11 (2009) 2129–2132.
[34] H.Y. Shen, H.M. Zheng, N. Zhu, Int. J. Electrochem. Sci. 5 (2010) 1587–1596.
[35] N. Li, Y. Ma, C. Yang, Biophys. Chem. 116 (2005) 199–205.
[36] L. Wang, P.F. Huang, J.Y. Bai, H.J. Wang, L.Y. Zhang, Y.Q. Zhao, Microchim. Acta 158 (2007) 151–157.
[37] J. Dong, X. Qu, L. Wang, C. Zhao, J. Xu, Electroanal 20 (2008) 1981–1986.
[38] S.J. Li, Y. Xing, G.F. Wang, Microchim. Acta 176 (2012) 163–168.
[39] Y. Ding, W. Liu, Q. Wu, X. Wang, J. Electroanal. Chem. 575 (2005) 275–280.
[40] M. Li, F. Ni, Y. Wang, S. Xu, D. Zhang, S. Chen, L. Wang, Electroanalysis 21 (2009) 1521–1526.
[41] X. Tian, Y. Song, H. Dong, Bioelectrochemistry 73 (2008) 18–22.
[42] A. Erdem, K. Kerman, B. Meric, Anal. Chim. Acta 422 (2000) 139–149.
[43] T. Luczak, Electrochim. Acta 53 (2008) 5725–5731.
[44] Y.H. Wu, S.S. Hu, Bioelectrochemistry 70 (2007) 335–341.
[45] E. Laviron, J. Electroanal, Chem. Interface Electrochem. 52 (1974) 355–393.
[46] A.J. Bard, L.R. Faulkner, Electrochemical Methods Fundamentals and Applications, Chemical Industry Press, Beijing, China (2005) 140.